

# Iron(II) and Cobalt(II) Complexes with 2,6-Bis(1,4-Diphenyl-5-Hydroxy-1*H*-Pyrazol-3-yl)pyridine: Synthesis, Structures, and Spin States

I. A. Nikovskii<sup>a</sup>, A. V. Polezhaev<sup>a, b</sup>, D. Yu. Aleshin<sup>a, c</sup>, E. K. Mel'nikova<sup>a, d</sup>,  
P. V. Dorovatovskii<sup>e</sup>, and Yu. V. Nelyubina<sup>a, f, \*</sup>

<sup>a</sup>Nesmeyanov Institute of Organoelement Compounds, Russian Academy of Sciences, Moscow, 119991 Russia

<sup>b</sup>Bauman State Technical University, Moscow, 107005 Russia

<sup>c</sup>Mendeleev University of Chemical Technology of Russia, Moscow, 125047 Russia

<sup>d</sup>Moscow State University, Moscow, 119899 Russia

<sup>e</sup>Kurchatov Institute Russian Research Center, Moscow, 123182 Russia

<sup>f</sup>Kurnakov Institute of General and Inorganic Chemistry, Russian Academy of Sciences, Moscow, 119991 Russia

\*e-mail: unelya@ineos.ac.ru

Received November 26, 2019; revised December 23, 2019; accepted December 24, 2019

**Abstract**—The reactions of 2,6-bis(1,4-diphenyl-5-hydroxy-1*H*-pyrazol-3-yl)pyridine (L), which is the first representative of a series of 2,6-bis(pyrazol-3-yl)pyridine ligands bearing substituents in positions 1 and 4 of the pyrazol-3-yl ring, with the divalent iron and cobalt salts afford new Co(II) and Fe(II) complexes:  $[\text{Co}(\text{L})_2](\text{ClO}_4)_2$  (**I**) and  $[\text{Fe}(\text{L})_2](\text{ClO}_4)_2$  (**II**). The compounds are isolated in the individual state and characterized by elemental analysis, NMR spectroscopy, and X-ray diffraction analysis (CIF files CCDC nos. 1967892 (**I**) and 1967893 (**II**)). According to the data obtained, the transition metal ion in complexes **I** and **II** exists in the high-spin state ( $S = 3/2$  for Co(II) and  $S = 2$  for Fe(II)) in a range of 120–345 K, and the proposed modification of the ligand does not lead to the temperature-induced spin transition in both the solution and crystalline state.

**Keywords:** bis(pyrazol-3-yl)pyridine, transition metal complexes, molecular design, X-ray diffraction analysis, spin transition

**DOI:** 10.1134/S1070328420050048

## INTRODUCTION

Bis(pyrazolyl)pyridines are actively used as ligands in complexes with various transition metals [1]. These complexes manifest a broad range of practically important properties, including catalytic (in cyclopropanation [2], epoxidation [3], and polymerization [4] reactions) and biological activity [5], and are among the most popular classes of molecular compounds [6] with spin transitions occurring upon the application of an appropriate external stimulus (temperature, pressure, light, magnetic and electric fields, etc.) [7, 8]. The latter property of the bis(pyrazolyl)pyridine complexes of transition metals (mainly iron(II)) allows using them in future quantum computers [9], molecular switches, sensors, and other molecular devices and materials [10–12].

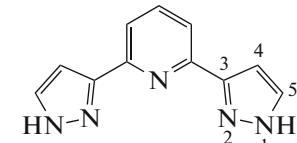
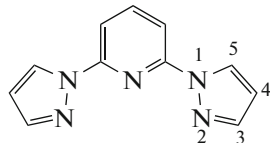
The ability to exist in two spin states is most often found in metal ions with the  $d^4$ – $d^7$  electronic configuration (e.g., Fe(II), Fe(III), or Co(II)) [7] in the (pseudo)octahedral coordination environment of

nitrogen-containing ligands, whose nature predetermines the possibility of transition between two states in the corresponding complex. However, the parameters of this transition depend, to a significant extent, on interactions between complex molecules, due to which a sharp spin transition with a hysteresis is possible in the crystalline sample [7]. Even slight changes “at the periphery” of the ligand can result in a change in the spin state of the metal ion [13, 14]. In some cases, the occurrence of the spin transition can be affected by the phase state of the studied compound (as a single crystal, polycrystalline powder, or in a solution) [15], polymorphic modification [16], and even solvent nature [16–18].

Necessary conditions for the target design of complexes with spin transitions satisfying requirements of their practical use in the molecular devices listed above [9–12] are systematic studies of series of compounds with structurally similar ligands in order to observe correlations between the substituent nature and spin transition parameters [19, 20]. Similar struc-

ture–property relationships were thus found for the Fe(II) complexes with the polydentate [21–30] ligands based on pyridine, including bis(pyrazolyl)pyridines [31]. Bis(pyrazolyl)pyridines can be

classified [1] as 2,6-bis(pyrazol-1-yl)pyridines and isomeric 2,6-bis(pyrazol-3-yl)pyridines (Scheme 1) differed by the method of conjunction of three heterocyclic fragments.

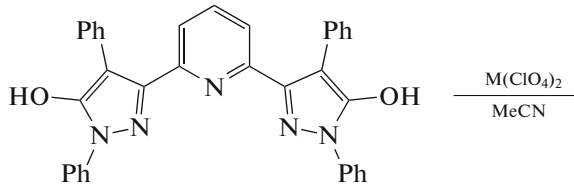


Scheme 1.

The earlier studies of the Fe(II) complexes with the 2,6-bis(pyrazol-1-yl)pyridine ligands [32], including those by NMR spectroscopy in a solution (Evans method) [33], made it possible to establish a distinct dependence of the spin state of the metal ion on the substituent position in the pyridine or pyrazolyl ring of the ligand and on its steric [6] and electronic [24] characteristics. Unfortunately, no similar relationships were observed for the complexes with isomeric 2,6-bis(pyrazol-3-yl)pyridines [6] because of the N–H···X hydrogen bonds formed by them with the coun-

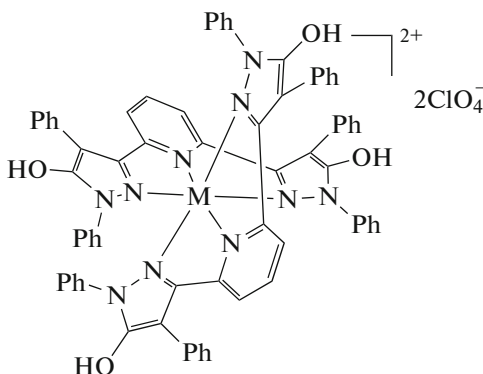
terions or solvent molecules, which unpredictably affect the spin state of the metal ion [16, 34–37].

A series of the Fe(II) and Co(II) bis(pyrazol-3-yl)pyridine complexes with phenyl substituents in position 1 of the pyrazol-3-yl ring has been synthesized previously in our laboratory (Scheme 1). These complexes stabilize the metal ion in the high-spin state [38, 39]. In this work, we synthesized new cobalt(II) (**I**) and iron(II) (**II**) complexes with the 2,6-bis(pyrazol-3-yl)pyridine ligand bearing phenyl substituents in positions 1 and 4 of the pyrazol-3-yl ring (Scheme 2).



I: M = Co(II)

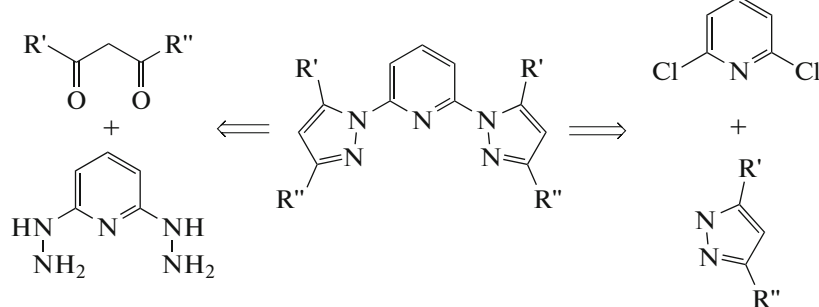
II: M = Fe(II)



Scheme 2.

Interestingly, the introduction of the substituent into a similar position of 3-substituted 2,6-bis(pyrazol-1-yl)pyridines, which can readily be derived from 2,6-dihydrazidopyridine and diketones [40] or from

2,6-dihalopyridines and 3,5-substituted pyrazoles (Scheme 3), afforded the Fe(II) complexes in the low-spin [6] or, on the contrary, high-spin [41] states.



Scheme 3.

At the same time, no modification of position 4 of the 2,6-bis(pyrazol-3-yl)pyridine ligands was carried out and, as a result, the influence of a similar substituent on the spin state of the metal ion has not been determined so far. For this purpose, we synthesized the first 1,4-tetraphenyl-substituted derivative of 2,6-bis(pyrazol-3-yl)pyridine, 2,6-bis(1,4-diphenyl-5-hydroxy-1*H*-pyrazol-3-yl)pyridine (**L**), and the corresponding homoleptic complexes **I** and **II**, whose spin states were determined by single-crystal X-ray diffraction of solvate complexes **I** and **II** at 120 K. The possibility of the spin transition to occur in a solution of the synthesized Fe(II) complex with temperature was studied using the Evans method [33], which is standard for these purposes and based on variable-temperature NMR spectroscopy.

## EXPERIMENTAL

All procedures related to the synthesis of the complexes were conducted in air using commercially available organic solvents distilled under argon. Compound  $\text{Fe}(\text{ClO}_4)_2 \cdot 6\text{H}_2\text{O}$  (Sigma-Aldrich) was used as received, and  $\text{Co}(\text{ClO}_4)_2 \cdot 6\text{H}_2\text{O}$  was synthesized using a described procedure [42]. The esterification of pyridine-2,6-dicarboxylic acid (Acros) with ethanol was carried out using a known procedure [43] in the presence of sulfuric acid. Analyses to carbon, nitrogen, and hydrogen were conducted on a Carlo Erba micro-analyzer (model 1106).

**Synthesis of diethyl-3,3'-(pyridine-2,6-diyl)bis(3-oxo-2-phenyl)propanoate.** Sodium hydride (1.8 g, 50 wt % suspension of NaH in mineral oil) was added to a mixture of diethyl pyridine-2,6-dicarboxylate (2.23 g, 10 mmol) and ethyl-2-phenylacetate (3.97 mL, 25 mmol) in anhydrous THF. The reaction mixture was refluxed with a reflux condenser for 4 h and then evaporated. A solid residue was washed with diethyl ether ( $2 \times 30$  mL). The residue was dried in vacuo and dispersed in water, and the obtained suspension was brought to pH 5 by the addition of 1 M hydrochloric acid. The resulting two-phase system was extracted with ethyl acetate, and the organic phase was separated, washed with distilled water, and dried over  $\text{Mg}_2\text{SO}_4$ . The drying agent was filtered off, and the mother liquor was evaporated. The obtained yellow oil was dissolved in a minor amount of diethyl ether and left at  $-20^\circ\text{C}$  for 2–3 days. The formed yellow precipitate was filtered off and dried in vacuo. The yield was 3.26 g (71%).

For  $\text{C}_{27}\text{H}_{25}\text{NO}_6$   
Anal. calcd., % C, 70.58 H, 5.48 N, 3.05  
Found, % C, 70.84 H, 5.68 N, 3.12

$^1\text{H}$  NMR (DMSO- $d_6$ , 400 MHz; mixture of keto and enol forms;  $\delta$ , ppm): 1.01–1.10 (t + t, 6H,  $2\text{CH}_3$ ), 3.41 (q, 4H,  $2\text{CH}_2$ ), 3.54 (s,  $\text{CH}_2$ , keto form), 4.10–

4.18 (q + q, 4H,  $\text{CH}_2$ ), 6.22 (q,  $\text{CH}_2$ , keto–enol form), 7.43–7.23 (m, 4Ph), 8.17–8.29 (m, Py).

**Synthesis of 2,6-bis(1,4-diphenyl-5-hydroxy-1*H*-pyrazol-3-yl)pyridine (**L**).** A mixture of diethyl-3,3'-(pyridine-2,6-diyl)bis(3-oxo-2-phenyl)propanoate (0.5 g, 1.09 mmol) and phenylhydrazine (246  $\mu\text{L}$ , 2.5 mmol) was dissolved in glacial acetic acid (10 mL). The obtained orange solution was refluxed with a reflux condenser for 8 h, after which the solution was cooled to room temperature and poured onto chipped ice (50 mL). The formed yellow precipitate was dissolved in a minimal amount of hot ethanol, and hot water was added by small portions to the obtained solution until a precipitate was formed. The resulting mixture was left at  $-10^\circ\text{C}$  for 12 h. The formed light yellow precipitate was filtered off, washed with water, and dried in vacuo. The yield was 489 mg (82%).

For  $\text{C}_{35}\text{H}_{25}\text{N}_5\text{O}_2$

Anal. calcd., % C, 76.77 H, 4.60 N, 12.79  
Found, % C, 76.93 H, 4.88 N, 12.90

$^1\text{H}$  NMR (DMSO- $d_6$ , 600 MHz;  $\delta$ , ppm): 7.20 (t, 2H,  $^3J_{\text{H},\text{H}} = 7.0$  Hz, *p*-Ph–H), 7.29 (m, 4H,  $^3J_{\text{H},\text{H}} = 7.0$  Hz, *m*-Ph–H), 7.35–7.37 (m, 6H, N-*p*-Ph–H + *o*-Ph–H), 7.53–7.55 (m, 6H, *m*-Ph–H + *m*-Py), 7.80 (t,  $^3J_{\text{H},\text{H}} = 7.8$  Hz, 1H, Py), 7.84–7.85 (m, 4H, N-*o*-Ph–H), 11.05 (s, 2H, OH,  $\text{D}_2\text{O}$ -exchangeable).

**Synthesis of  $[\text{Co}(\text{L})_2](\text{ClO}_4)_2$  (**I**).** Weighed samples of  $\text{Co}(\text{ClO}_4)_2 \cdot 6\text{H}_2\text{O}$  (0.026 g, 0.1 mmol) and **L** (0.109 g, 0.2 mmol) were mixed in acetonitrile. The obtained solution was stirred for 3 h, and diethyl ether was added until a precipitate was formed. The mixture was left to crystallize at  $-10^\circ\text{C}$  for 12 h. The formed finely crystalline powder was filtered off and dried in vacuo to a constant weight. The yield was 244 mg (91%).

For  $\text{C}_{70}\text{H}_{50}\text{N}_{10}\text{O}_{12}\text{Cl}_2\text{Co}$   
Anal. calcd., % C, 62.14 H, 3.72 N, 10.35  
Found, % C, 62.27 H, 3.78 N, 10.43

$^1\text{H}$  NMR (CD<sub>3</sub>CN; 600 MHz;  $\delta$ , ppm): –1.74 (br.s, 2H, *p*-Py–H), 2.10 (br.s, 4H, N-*p*-Ph–H), 2.60 (br.s, 8H, N-*m*-Ph–H), 7.34 (br.s, 4H, *p*-Ph–H), 8.29 (br.s, 8H, *m*-Ph–H), 9.23 (br.s, 8H, *o*-Ph–H), 16.97 (br.s, 8H, N-*o*-Ph–H), 26.94 (br.s, 4H, *m*-Py–H), 30.97 (br.s, 4H, OH).

**Synthesis of  $[\text{Fe}(\text{L})_2](\text{ClO}_4)_2$  (**II**).** Weighed samples of  $\text{Fe}(\text{ClO}_4)_2 \cdot 6\text{H}_2\text{O}$  (0.036 g, 0.1 mmol) and **L** (0.109 g, 0.2 mmol) were mixed in acetonitrile, the resulting solution was stirred for 3 h, and hexane was added until a precipitate was formed. The formed

**Table 1.** Main crystallographic data and structure refinement parameters for compounds **I**·2.5THF and **II**·3.75THF·1.5Et<sub>2</sub>O

Parameter	Value	
	<b>I</b> ·2.5THF	<b>II</b> ·3.75THF·1.5Et <sub>2</sub> O
Empirical formula	C <sub>80</sub> H <sub>70</sub> N <sub>10</sub> O <sub>14.5</sub> Cl <sub>2</sub> Co	C <sub>91</sub> H <sub>95</sub> N <sub>10</sub> O <sub>17.25</sub> Cl <sub>2</sub> Fe
<i>FW</i>	1533.29	1731.51
<i>T</i> , K	120	120
Crystal system	Orthorhombic	Monoclinic
Space group	<i>Pccn</i>	<i>P2<sub>1</sub>/c</i>
<i>Z</i>	8	4
<i>a</i> , Å	53.674(7)	21.322(4)
<i>b</i> , Å	14.7409(18)	13.518(3)
<i>c</i> , Å	20.047(3)	30.498(6)
<i>V</i> , Å <sup>3</sup>	15 861(3)	8777(3)
ρ <sub>calc</sub> , g cm <sup>-3</sup>	1.284	1.310
μ, cm <sup>-1</sup>	3.53	4.24
<i>F</i> (000)	6376	3636
2θ <sub>max</sub> , deg	60	60
Number of measured reflections	187091	90933
Number of independent reflections	24270	19114
Number of reflections with <i>I</i> > 3σ( <i>I</i> )	8060	12514
Number of refined parameters	1108	1135
<i>R</i> <sub>1</sub> , <i>wR</i> <sub>2</sub> ( <i>I</i> > 2σ( <i>I</i> ))	0.1337, 0.3482	0.1047, 0.2616
<i>R</i> <sub>1</sub> , <i>wR</i> <sub>2</sub> (over all data)	0.2911, 0.4234	0.1465, 0.2945
GOOF	1.041	1.031
Residual electron density, (max/min), e Å <sup>-3</sup>	1.237/−0.655	1.039/−0.705

finely crystalline powder was dried in vacuo to a constant weight. The yield was 244 mg (91%).

For C<sub>70</sub>H<sub>50</sub>N<sub>10</sub>O<sub>12</sub>Cl<sub>2</sub>Fe

Anal. calcd., % C, 62.28 H, 3.73 N, 10.38  
Found, % C, 62.11 H, 3.44 N, 10.13

<sup>1</sup>H NMR (CD<sub>3</sub>CN; 600 MHz; δ, ppm): −9.21 (br.s, 8H, *m*-Ph—H/*o*-Ph—H), 8.67 (br.s, 4H, *p*-Ph—H), 8.87 (br.s, 8H, *m*-Ph—H/*o*-Ph—H), 9.10 (br.s, 8H, *m*-Ph—H/*o*-Ph—H), 9.68 (br.s, 8H, *m*-Ph—H/*o*-Ph—H), 11.57 (br.s, 4H, *p*-Ph—H), 18.33 (br.s, 4H, OH), 27.74 (br.s, 2H, *p*-Py—H), 60.68 (br.s, 4H, *m*-Py—H).

**X-ray diffraction analysis (XRD).** The XRD study of the single crystals of compound **I**·2.5THF, which were obtained by the slow evaporation of complex **I** in air from a THF solution, was carried out on a Bruker APEX 2 CCD diffractometer (MoK<sub>α</sub> radiation, graphite monochromator, ω scan mode). A set of XRD data for the single crystals of compound **II**·3.75THF·1.5Et<sub>2</sub>O, which were formed due to the diffusion of Et<sub>2</sub>O vapors into a solution of complex **II** in THF, was

obtained at the protein crystallography station of the Kurchatov Synchrotron Radiation Center (λ = 0.9699 Å). The structures were solved using the ShelXT program [44] and refined by full-matrix least squares using the Olex 2 program [45] in the anisotropic approximation for *F*<sub>hkl</sub><sup>2</sup>. The hydrogen atoms of the OH groups were localized from the difference Fourier electron density syntheses, and positions of other hydrogen atoms were calculated geometrically. All hydrogen atoms were refined in the isotropic approximation by the riding model. The main crystallographic data and structure refinement parameters are presented in Table 1.

The structural data for compounds **I**·2.5THF and **II**·3.75THF·1.5Et<sub>2</sub>O were deposited with the Cambridge Crystallographic Data Centre (CIF files CCDC nos. 1967892 and 1967893, respectively; <http://www.ccdc.cam.ac.uk/>).

**NMR spectroscopy.** <sup>1</sup>H NMR spectra were recorded for solutions of complexes **I** and **II** in DMSO-d<sub>6</sub> and CD<sub>3</sub>CN on Bruker Avance 300, Bruker Avance 400, and Bruker Avance 600 spectrometers with working frequencies of 300.15, 400, and 600.22 MHz,

respectively. Chemical shifts ( $\delta$ , ppm) in the spectra were determined relative to the residual signal of the solvent ( $^1\text{H}$  2.5 ppm for  $\text{DMSO-d}_6$  and  $^1\text{H}$  1.94 ppm for  $\text{CD}_3\text{CN}$ ).  $^1\text{H}$  NMR spectra were recorded using the following parameters: spectral range 1000 ppm, detection time 0.1 s, relaxation delay 0.1 s, pulse duration 6.5  $\mu\text{s}$ , and acquisition number 1024.

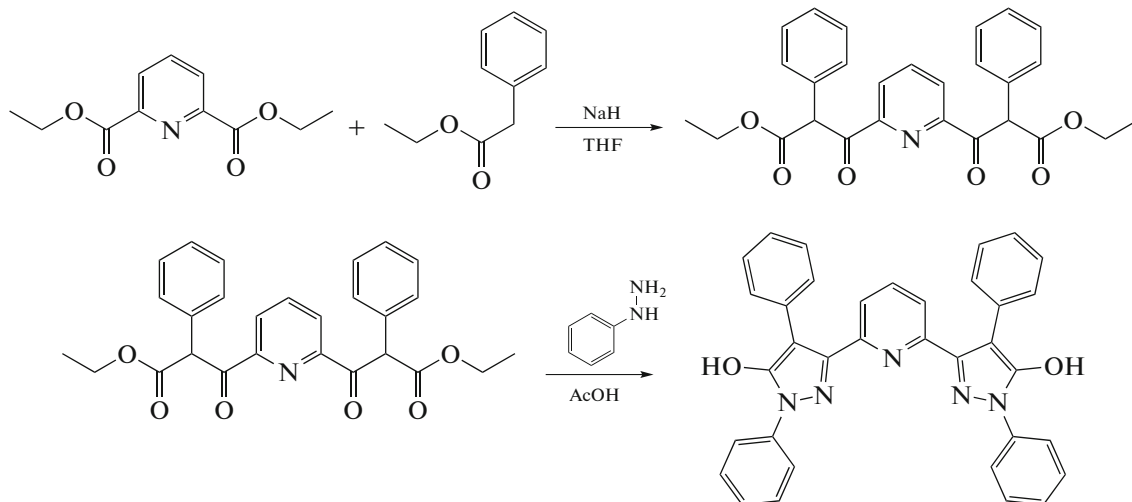
**Evans method.** The temperature dependence of the molar magnetic susceptibility ( $\chi_M$ ) of the iron(II) complex in a deuterated acetonitrile solution was evaluated by the Evans method [33] on the basis of the  $^1\text{H}$  NMR spectra recorded in a range of 235–345 K using a NMR tube with a coaxial inset. The inner (control) tube was filled with  $\text{CH}_3\text{CN-d}_3$  with an additive of ~1%  $\text{Me}_4\text{Si}$ , and the outer tube contained a solution of the complex (~1–5 mg/cm<sup>3</sup>) in  $\text{CH}_3\text{CN-d}_3$  with the same concentration of  $\text{Me}_4\text{Si}$ . The value of  $\chi_M$  was calculated from the difference between the chemical shifts of  $\text{Me}_4\text{Si}$  in pure  $\text{CH}_3\text{CN-d}_3$  and in a solution of the complex ( $\Delta\delta$ , Hz) in  $\text{CH}_3\text{CN-d}_3$  using the following equation:

$$\chi_M = \frac{\Delta\delta M}{v_0 S_f c} - \chi_M^{\text{dia}},$$

where  $M$  is the molar mass of the iron(II) complex, g/mol;  $v_0$  is the spectrometer frequency, Hz;  $S_f$  is the coefficient of the magnet shape ( $4\pi/3$ );  $c$  is the concentration of the complex, g/cm<sup>3</sup>; and  $\chi_M^{\text{dia}}$  is the molar diamagnetic contribution to the paramagnetic susceptibility calculated using Pascal's constants [46]. The concentration ( $c$ ) was recalculated for each temperature according to a change in the solvent density ( $\rho$ ):  $c_T = m_c \rho / m_{\text{sol}}$ , where  $m_c$  is the weight of the complex, and  $m_{\text{sol}}$  is the weight of the solution.

## RESULTS AND DISCUSSION

New ligand L with phenyl groups in positions 1 and 4 of the pyrazol-3-yl rings (Scheme 4) was synthesized using the modified procedure earlier developed for the synthesis of 2,6-bis(1-phenyl-5-hydroxy-1*H*-pyrazol-3-yl)pyridines [43]. Bis( $\beta$ -keto ester) was obtained as a mixture of tautomers by the mixed Claisen condensation between diethyl-2,6-pyridinedicarboxylate and ethyl phenylacetate in the presence of sodium hydride in a THF solution. The obtained product was subjected to cyclization in the presence of phenylhydrazine (2 equiv) in acetic acid to form ligand L in a high yield.



Scheme 4.

Complexes **I** and **II** with synthesized ligand L were obtained in high yields from cobalt(II) and iron(II) perchlorate hydrates by the direct template reaction in acetonitrile at room temperature (Scheme 2). Both complexes were isolated in the individual state and characterized by elemental analysis, NMR spectroscopy, and XRD.

The appropriate single crystals of complexes **I** and **II** (Fig. 1) were prepared by the recrystallization of the powdered samples from THF solutions as solvates **I**·2.5THF and **II**·3.75THF·1.5Et<sub>2</sub>O, respectively. In the second case, the crystal also contains 1.5 diethyl

ether molecules per molecule of complex **II** due to Et<sub>2</sub>O vapor diffusion to the solution of the complex in THF (see Experimental).

The molecules of the indicated solvents “trapped” during the crystallization of compounds **I**·2.5THF and **II**·3.75THF·1.5Et<sub>2</sub>O form hydrogen bonds with three hydroxyl groups of two bis(pyrazol-3-yl)pyridine ligands L (O···O 2.556(10)–2.615(6) Å, OH–O angle 152(1)°–162(1)°), whereas their fourth hydroxyl group is involved in hydrogen bonding with the perchlorate anions (O···O 2.576(14)–2.720(17) Å, OH–O angle 126(1)°–158(1)°).

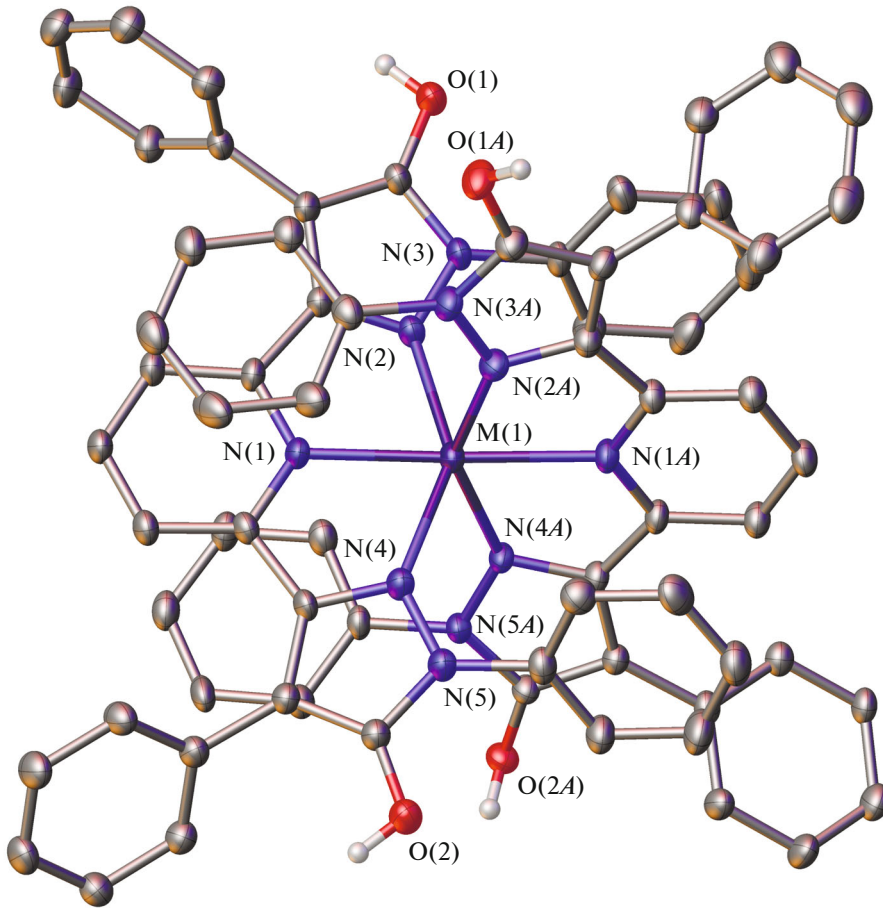


**Fig. 1.** General view of complexes **I** ( $M = \text{Co}$ ) and **II** ( $M = \text{Fe}$ ) in the crystals of **I**·2.5THF and **II**·3.75THF·1.5Et<sub>2</sub>O in the representation of atoms by thermal vibration ellipsoids ( $p = 50\%$ ). The perchlorate anions, disordered solvent molecules, and hydrogen atoms, except for those belonging to the OH groups, are omitted.

Two bis(pyrazol-3-yl)pyridine ligands are coordinated to the transition metal ion by three nitrogen atoms (coordination number 6) with the distances (Table 2) typical of the cobalt(II) and iron(II) ions in the high-spin state (2.0–2.2 Å [7]). The latter also follows from the trigonal prismatic distortion of the coordination  $MN_6$  polyhedron ( $M = \text{Co, Fe}$ ) [47], which is an octahedron in the case of the low-spin transition metal ion with the  $d^7$  configuration. In particular, the  $N(\text{Py})MN(\text{Py})$  angle and dihedral  $\theta$  angle between the route-mean-square planes of two ligands (Fig. 2), which are equal to 90° and 180° in the case of an ideal octahedron, are 69.35(5)° and 177.8(2)° in the crystal of **I**·2.5THF and 70.66(4)° and 177.74(15)° in the crystal of **II**·3.75THF·1.5Et<sub>2</sub>O. The observed trigonal prismatic geometry of the N(6)-environment of the metal ion is a consequence of both the “rigidity” of the 2,6-bis(pyrazol-3-yl)pyridine ligand [47] and also the bulky phenyl substituents in position 1 of the pyrazol-3-yl cycle. For comparison, similar values of the  $N(\text{Py})MN(\text{Py})$  and  $\theta$  angles for the earlier described Co(II) [39] and Fe(II) [38] complexes with *N,N'*-diphenyl-substituted

diphenyl-substituted bis(pyrazol-3-yl)pyridines lied in ranges of 67.5(3)°–68.3(3)° and 176.1(2)°–180°, respectively.

A similar distortion of the coordination  $MN_6$  polyhedron characteristic of the high-spin metal complexes with the bi- and tridentate ligands [48] can graphically be presented as so-called “continuous symmetry measures” [48] describing deviations from an ideal octahedron (S(OC-6)) and an ideal trigonal prism (S(TP-6)). The lower the deviation values, the closer the shape of the coordination polyhedron to the corresponding polyhedron. In the case of the studied single crystals of compounds **I**·2.5THF and **II**·3.75THF·1.5Et<sub>2</sub>O, the octahedral S(OC-6) and trigonal prismatic S(TP-6) “continuous symmetry measures” (Fig. 3) estimated from the XRD data are 4.832–6.123 and 10.797–11.015 (Table 2), indicating a noticeable distortion of the coordination  $MN_6$  polyhedron toward a trigonal prism. They fall onto the range of the S(OC-6) and S(TP-6) “continuous symmetry measures” characteristic of the high- Co(II) [39] and Fe(II) [38] complexes with *N,N'*-diphenyl-substituted

**Table 2.** Selected geometric parameters for solvate complexes **I** and **II** according to the XRD data at 120 K\*

Parameter	Value	
	<b>I</b> ·2.5THF	<b>II</b> ·3.75THF·1.5Et <sub>2</sub> O
M—N(Py), Å	2.079(5)/2.081(5)	2.158(3)/2.159(3)
M—N(Pz), Å	2.134(6)–2.178(6)	2.211(4)–2.207(4)
θ, deg	69.35(5)	70.66(4)
N(Py)MN(Py), deg	177.8(2)	177.74(15)
α, deg	56.8(2)–67.50(18)	60.68(14)–66.45(15)
δ, deg	51.8(2)–64.2(2)	61.76(15)–83.01(14)
S(TP-6)	10.797	11.015
S(OC-6)	4.832	6.123

\* θ is the dihedral angle between the root-mean-square planes of the 2,6-bis(pyrazol-3-yl)pyridine ligands, the N(Py) and N(Pz) atoms correspond to the nitrogen atoms of the pyridine and pyrazol-3-yl fragments, α and δ correspond to the rotation angles of the phenyl substituents in positions 1 and 4 of the pyrazol-3-yl fragment relative to its plane, and S(TP-6) and S(OC-6) are deviations of the MN<sub>6</sub> polyhedron from an ideal trigonal prism (TP-6) and an ideal octahedron (OC-6), respectively.

bis(pyrazol-3-yl)pyridines. The rotation angles of the phenyl groups in position 1 of the pyrazol-3-yl cycle in compounds **I**·2.5THF and **II**·3.75THF·1.5Et<sub>2</sub>O, being equal to 56.8(2)°–67.50(18)°, also differ slightly from the corresponding values (42.7(2)°–66.4(2)°) in the mentioned complexes of Co(II) [39] and Fe(II) [38]. Interestingly, the phenyl substituents in position 4 of the pyrazol-3-yl cycle in compounds **I**·2.5THF and **II**·3.75THF·1.5Et<sub>2</sub>O turn out to be rotated relative to the plane of this cycle to the same extent or even strongly (Table 2), which can be related to the steric effect of the closely arranged pyridine fragment of ligand L.

Thus, the XRD data unambiguously indicate that the cobalt(II) and iron(II) ions in the synthesized solvate complexes **I**·2.5THF and **II**·3.75THF·1.5Et<sub>2</sub>O with significant trigonal prismatic distortions of the

(pseudo)octahedral environment of the transition metal ion exist in the high-spin state at 120 K.

The cobalt(II) ion in the (pseudo)octahedral environment of two 2,6-bis(pyrazol-3-yl)pyridine ligands exists in the high-spin state [49, 50] due to the ligand field formed by them, while the absence of the temperature-induced transition in the solution of the synthesized Fe(II) complex is confirmed by the data of the Evans method [33]. This method based on the use of widely available NMR spectroscopy is one of the most popular approaches that makes it possible to

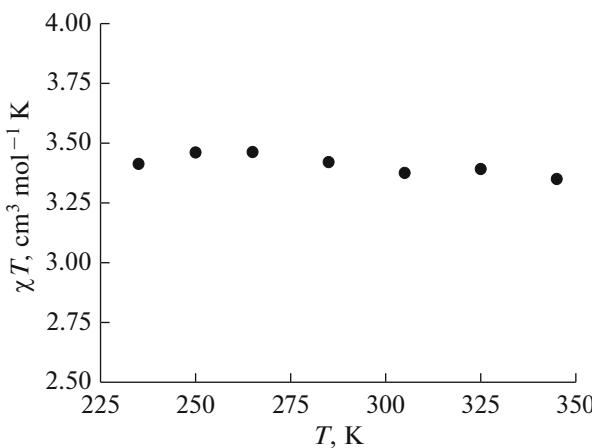


**Fig. 2.** Temperature dependence of the magnetic susceptibility of complex **II** in a deuterated acetonitrile solution according to the NMR spectroscopic data (Evans method).

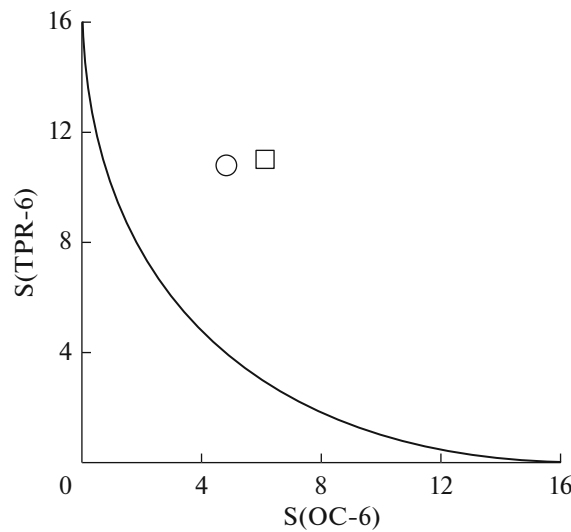


**Fig. 3.** Graphical representation of the S(TP-6) and S(OC-6) “continuous symmetry measures” as deviations of the MN<sub>6</sub> polyhedron in the crystals of (○) **I**·2.5THF and (□) **II**·3.75THF·1.5Et<sub>2</sub>O from an ideal trigonal prism (TP-6) and an ideal octahedron (OC-6), respectively. Black line shows the route of the least distortion of the polyhedron geometry on going between the indicated polyhedra.

measure the magnetic susceptibility of the solution and thus directly determine the spin state of the metal ion. The essence of the method is that the addition of a paramagnetic compound, such as the Co(II) or Fe(II) complex in the high-spin state, to the solution changes the magnetic susceptibility of the whole solution. This results in a change in the chemical shifts of the nuclei in the NMR spectra, which can quantitatively be estimated by the simultaneous detection of the NMR spectra for a solution of the standard diamagnetic compound, for example, tetramethylsilane (TMS), in the presence and in the absence of the paramagnetic complex. For this purpose, a special coaxial inset containing a TMS solution in a solvent is placed in an NMR tube containing a solution of TMS and the corresponding complex in the known concentration in the same deuterated solvent. The final  $^1\text{H}$  NMR spectrum exhibits two signals from the TMS protons: one signal is from the pure solution in the coaxial inset, and the second signal is from the solution with an additive of the paramagnetic complex in the NMR tube. The observed difference in the chemical shifts of the TMS protons in two solutions makes it possible to calculate the magnetic susceptibility of the studied paramagnetic compound (see Experimental) and thus unambiguously determine the spin state of the metal ion at a certain temperature or in a temperature range in a chosen solvent.

Deuterated acetonitrile was used as such a solvent for the measurement of the magnetic susceptibility of bis(pyrazol-3-yl)pyridine complex **II**, since the dissolution in this solvent gave no precipitate even on cooling the obtained solution to 235 K. The latter is the necessary condition for the reliable determination of the spin state of the metal ion using the Evans method, since the concentration of the paramagnetic compound, which is a term of the equation for the calculation of the magnetic susceptibility, can change in the opposite case.

According to the data obtained, the value of  $\chi T$  for complex **II** (Fig. 2) in deuterated acetonitrile at 235–345 K is  $3.4 \text{ cm}^3 \text{ mol}^{-1} \text{ K}$  in the whole temperature range, which unambiguously indicates the high-spin state of the iron(II) ion ( $S = 2$ ). In turn, this indicates that the absence of a temperature-induced spin transition in the complexes with ligand L has the “intramolecular” nature, which can be related, in the case of the Fe(II) complex, to the phenyl substituents in position 1 of the pyrazol-3-yl ring [38]. The Co(II) complex exists only in the high-spin state in the (pseudo)octahedral environment of two 2,6-bis(pyrazol-3-yl)pyridine ligands, whose field does not allow the cobalt(II) ion to transfer to the low-spin state with temperature [49, 50].

Thus, we synthesized and characterized new Co(II) and Fe(II) complexes with the first representative of the series of 2,6-bis(pyrazol-3-yl)pyridines containing substituents simultaneously in positions 1

and 4 of the pyrazol-3-yl ring. The low-temperature XRD data obtained for them, first of all, the M–N bond lengths and trigonal prismatic distortion of the coordination  $\text{MN}_6$  polyhedron unambiguously indicate that the cobalt(II) and iron(II) ions in the crystals of compounds **I**·2.5THF and **II**·3.75THF·1.5Et<sub>2</sub>O at 120 K exist in the high-spin state ( $S = 3/2$  for Co(II) and  $S = 2$  for Fe(II)). The absence of the temperature-induced spin transition in the solution is also confirmed by the NMR spectroscopic data (Evans method) for the Fe(II) complex in a range of 235–345 K. Thus, the proposed modification of the ligand by the introduction of an additional phenyl substituent into position 4 of the pyrazol-3-yl ring with the bulky phenyl groups in position 1 exerts no effect on the spin state of the cobalt(II) and iron(II) ions in the corresponding complexes, which remain high-spin in both the crystalline state and solution.

## ACKNOWLEDGMENTS

The XRD data were performed with the financial support from Ministry of Science and Higher Education of the Russian Federation using the equipment of Center for molecular composition studies of INEOS RAS.

## FUNDING

This work was supported by the Russian Science Foundation, project no. 17-13-01456.

## CONFLICT OF INTEREST

The authors declare that they have no conflicts of interest.

## REFERENCES

1. Halcrow, M.A., *Coord. Chem. Rev.*, 2005, vol. 249, no. 24, p. 2880.
2. Christenson, D.L., Tokar, C.J., and Tolman, W.B., *Organometallics*, 1995, vol. 14, no. 5, p. 2148.
3. Fung, W.-H., Cheng, W.-C., Yu, W.-Y., et al., *J. Chem. Soc., Chem. Commun.*, 1995, no. 19, p. 2007.
4. Zikode, M., Ojwach, S.O., and Akerman, M.P., *J. Mol. Catal. A*, 2016, vol. 413, p. 24.
5. Hopa, C., Yildirim, H., Kara, H., et al., *Spectrochim. Acta, Part A*, 2014, vol. 121, p. 282.
6. Halcrow, M.A., *Crystals*, 2016, vol. 6, no. 5, p. 58.
7. *Spin-Crossover Materials: Properties and Applications*, Halcrow, M.A., Ed., New York: Wiley, 2013.
8. Gülich, P., Gaspar, A.B., and Garcia, Y., *Beilstein J. Org. Chem.*, 2013, vol. 9, p. 342.
9. Ferrando-Soria, J., Vallejo, J., Castellano, M., et al., *Coord. Chem. Rev.*, 2017, vol. 339, p. 17.
10. Hayami, S., Holmes, S.M., and Halcrow, M.A., *J. Mat. Chem.*, 2015, vol. 3, no. 30, p. 7775.
11. Molnár, G., Rat, S., Salmon, L., et al., *Adv. Mater.*, 2017, vol. 30, no. 5, p. 1703862.

12. Senthil Kumar, K. and Ruben, M., *Coord. Chem. Rev.*, 2017, vol. 346, p. 176.
13. Judge, J.S. and Baker, W., *Inorg. Chim. Acta*, 1967, vol. 1, p. 68.
14. Harris, C., Lockyer, T., Martin, R., et al., *Aust. J. Chem.*, 1969, vol. 22, no. 10, p. 2105.
15. Novikov, V.V., Ananyev, I.V., Pavlov, A.A., et al., *J. Phys. Chem. Lett.*, 2014, vol. 5, no. 3, p. 496.
16. Bartual-Murgui, C., Codina, C., Roubeau, O., and Aromi, G., *Chem.-Eur. J.*, 2016, vol. 22, no. 36, p. 12767.
17. Hathcock, D.J., Stone, K., Madden, J., and Slattery, S.J., *Inorg. Chim. Acta*, 1998, vol. 282, no. 2, p. 131.
18. Constable, E.C., Housecroft, C.E., Kulke, T., et al., *Dalton Trans.*, 2001, no. 19, p. 2864.
19. Kershaw Cook, L.J., Kulmaczewski, R., Mohammed, R., et al., *Angew. Chem., Int. Ed. Engl.*, 2016, vol. 55, no. 13, p. 4327.
20. Pavlov, A.A., Aleshin, D.Y., Nikovskiy, I.A., et al., *Eur. J. Inorg. Chem.*, 2019, vol. 2019, no. 23, p. 2819.
21. Phan, H., Hrudka, J.J., Igimbayeva, D., Lawson Daku, L.M., and Shatruk, M., *J. Am. Chem. Soc.*, 2017, vol. 139, no. 18, p. 6437.
22. Rodríguez-Jiménez, S., Yang, M., Stewart, I., et al., *J. Am. Chem. Soc.*, 2017, vol. 139, no. 50, p. 18392.
23. Kimura, A. and Ishida, T., *ACS Omega*, 2018, vol. 3, no. 6, p. 6737.
24. Kershaw Cook, L.J., Kulmaczewski, R., Mohammed, R., et al., *Angew. Chem., Int. Ed. Engl.*, 2016, vol. 55, no. 13, p. 4327.
25. Elhaïk, J., Evans, D.J., Kilner, C.A., and Halcrow, M.A., *Dalton Trans.*, 2005, no. 9, p. 1693.
26. McPherson, J.N., Elton, T.E., and Colbran, S.B., *Inorg. Chem.*, 2018, vol. 57, no. 19, p. 12312.
27. Santoro, A., Kershaw Cook, L.J., Kulmaczewski, R., et al., *Inorg. Chem.*, 2015, vol. 54, no. 2, p. 682.
28. Nakano, K., Suemura, N., Yoneda, K., et al., *Dalton Trans.*, 2005, no. 4, p. 740.
29. Kitchen, J.A., Olguin, J., Kulmaczewski, R., et al., *Inorg. Chem.*, 2013, vol. 52, no. 19, p. 11185.
30. Hoselton, M.A., Wilson, L.J., and Drago, R.S., *J. Am. Chem. Soc.*, 1975, vol. 97, no. 7, p. 1722.
31. Hamon, P., Thepot, J.Y., Le Floch, M., et al., *Angew. Chem., Int. Ed. Engl.*, 2008, vol. 47, p. 8687.
32. Halcrow, M.A., *Coord. Chem. Rev.*, 2009, vol. 253, no. 21, p. 2493.
33. Evans, D.F., *J. Chem. Soc. (Resumed)*, 1959, p. 2003.
34. Scudder, M.L., Craig, D.C., and Goodwin, H.A., *CrystEngComm*, 2005, vol. 7, no. 107, p. 642.
35. Clemente-León, M., Coronado, E., Giménez-López, M.C., and Romero, F.M., *Inorg. Chem.*, 2007, vol. 46, no. 26, p. 11266.
36. Coronado, E., Giménez-López, M.C., Giménez-Saiz, C., and Romero, F.M., *CrystEngComm*, 2009, vol. 11, no. 10, p. 2198.
37. Jornet-Molla, V., Giménez-Saiz, C., and Romero, F.M., *Crystals*, 2018, vol. 8, p. 439.
38. Nelyubina, Y.V., Polezhaev, A.V., Pavlov, A.A., et al., *Magnetochemistry*, 2018, vol. 4, no. 4, p. 46.
39. Pavlov, A.A., Belov, A.S., Savkina, S.A., et al., *Russ. J. Coord. Chem.*, 2018, vol. 44, p. 489. <https://doi.org/10.1134/S1070328418080067>
40. Jackson, M.T., Spiegel, M., Farmer, P.J., et al., *Inorg. Chim. Acta*, 2018, vol. 473, p. 180.
41. Jackson, M.T., Spiegel, M., Farmer, P.J., et al., *Inorg. Chim. Acta*, 2018, vol. 473, p. 180.
42. Hynes, M.J. and O'Shea, M.T., *J. Chem. Soc., Dalton Trans.*, 1983, no. 2, p. 331.
43. Polezhaev, A.V., Chen, C.-H., Kinne, A.S., et al., *Inorg. Chem.*, 2017, vol. 56, no. 16, p. 9505.
44. Sheldrick, G.M., *Acta Crystallogr., Sect. A: Found. Crystallogr.*, 2008, vol. 64, p. 112.
45. Dolomanov, O.V., Bourhis, L.J., Gildea, R.J., et al., *J. Appl. Crystallogr.*, 2009, vol. 42, p. 339.
46. Bain, G.A. and Berry, J.F., *J. Chem. Educ.*, 2008, vol. 85, no. 4, p. 532.
47. Alvarez, S., *J. Am. Chem. Soc.*, 2003, vol. 125, no. 22, p. 6795.
48. Alvarez, S., *Chem. Rev.*, 2015, vol. 115, p. 13447.
49. Holland, J.M., Kilner, C.A., Thornton-Pett, M., and Halcrow, M.A., *Polyhedron*, 2001, vol. 20, no. 22, p. 2829.
50. Cook, L. and Halcrow, M.A., *Magnetochemistry*, 2015, vol. 1, p. 3.

Translated by E. Yablonskaya